

A Novel Triazole Nucleoside Suppresses Prostate Cancer Cell Growth by Inhibiting Heat Shock Factor 1 and Androgen Receptor

Yi Xia^{a,b,*}, Menghua Wang^{c,d}, Eliana Beraldi^a, Mei Cong^c, Amina Zoubeidi^a, Martin Gleave^a and Ling Peng^{c,*}

^a The Vancouver Prostate Centre, University of British Columbia, Vancouver, Canada; ^b Innovative Drug Research Centre, Chongqing University, Chongqing, China; ^c Centre Interdisciplinaire de Nanoscience de Marseille, CNRS UMR 7325, Aix-Marseille Université Marseille, France; ^d College of Chemistry and Molecular Sciences, Wuhan University, Wuhan, China.

Abstract: A novel triazole nucleoside analogue was discovered to exhibit potent anticancer activity in prostate cancer cells via down-regulating heat shock factor 1 (HSF1) and related heat shock proteins, along with the consequential inhibition of androgen receptor (AR) expression and transactivation, arresting the cell cycle in AR-governed phase. This triazole nucleoside therefore constitutes a novel structural paradigm and potential drug candidate for prostate cancer through inhibition of HSF1 and AR.

Keywords: Androgen receptor, anticancer activity, heat shock proteins, heat shock factor 1, nucleoside analogues, prostate cancer.

1. INTRODUCTION

Prostate cancer (PCa) is a major health problem of the 21st century and one of the most commonly diagnosed cancers for elder men in developed countries[1, 2]. While PCa initially responds to first-line androgen deprivation therapy (ADT), resistance occurs with time and most patients eventually develop castration-resistant prostate cancer (CRPC), a malignant disease without curative therapy[3]. CRPC is often characterized by the reactivation of androgen receptor (AR), a phosphoprotein acting as a ligand-activated transcription factor[4, 5]. AR signaling mediates cell growth, proliferation, differentiation, and homeostasis for prostate cancer development[5]. Regarding the crucial role of AR-signaling pathway for tumor growth in castrate environment, inhibiting AR constitutes one of the most efficient ways in CRPC therapy[6, 7].

In AR signaling, AR is bound to heat shock protein (HSPs) complex to maintain AR in a stable and mature conformation with high affinity to androgen[4]. Consequently, targeting HSPs such as HSP27 and HSP90 is able to inhibit AR activity[8, 9]. Moreover, compared to traditional antiandrogen treatment, inhibition of HSPs does not induce agonistic effect[10] nor be conferred resistance with spliced variants of AR[11]. In addition, HSPs also have cytoprotective roles for multiple oncoproteins and regulate their cellular signaling and transcriptional functions, hence to

promote prostate carcinogenesis and progression[8, 10]. In the past years, different strategies that address the AR-associated HSPs as novel targets have been developed for PCa therapy including small-molecular inhibitors for HSP90[9, 12] and antisense oligonucleotides for HSP27[13] and clusterin[14]. They simultaneously target multiple oncogenic pathways to delay CRPC tumor growth. Encouraged by these results, searching for novel drug candidates to target AR via inhibition of HSPs is of great interest for fighting against CRPC.

Recently, we have discovered a triazole nucleoside **WJQ-101** (Figure 1) that down-regulates HSP27[15]. Its optimized analogue **Ly101-4B** (Figure 1) even suppresses heat shock factor 1 (HSF1)-mediated heat shock response (HSR) pathways to yield a more powerful antitumoral activity against drug-resistant pancreatic cancer [16, 17]. HSF1 is the most significant HSR regulator, which transcriptionally regulates stress inducible HSPs and participates in numerous other signaling and metabolic pathways to promote cell survival[18]. Suppression of HSF1 therefore can coincidentally down-regulate multiple HSPs such as HSP27,

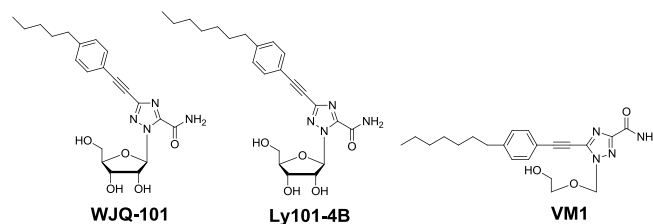


Fig. (1). Triazole nucleosides **WJQ-101**, **Ly101-4B** and **VM1**.

*Address correspondence to these authors at CNRS UMR 7325, Aix-Marseille Université Marseille, France; Tel: ++33491829154, Fax: ++33491829154; E-mail: ling.peng@univ-amu.fr and Innovative Drug Research Centre, Chongqing University, Chongqing, China; Tel/Fax: ++862365678457; E-mail: yixia@cqu.edu.cn

HSP70 and HSP90. Concerning the master role of HSF1 for HSPs and the involvement of HSPs in AR signaling, we surmised that triazole nucleoside analogues that can down-regulate HSF1 might also exhibit inhibitory effect on AR expression in PCa. We therefore screened a variety of triazole nucleosides previously developed by us[19].

These compounds bear aromatic moieties appended on the heterocyclic triazolenucleobase that may enhance interaction with their biological targets[19]. Most importantly, we identified the acyclic analogue **VM1** (Figure 1) which was more efficacious to down-regulate HSF1 and, at the same time, to suppress AR activity, leading to potent caspase-dependent apoptosis in various PCa cell lines. Compound **VM1** shares some similar structural feature as in **WJQ-101** and **Ly101-4B** such as the long phenyl alkyl chain appended on the triazole ring. It also exhibits structural difference such as the acyclic sugar component and the 5-isomeric constitution of the appendage on the triazole instead of the cyclic ribose sugar entity and the 3-isomeric constitution in **WJQ-101** and **Ly101-4B**. This finding provides a new structural motif in search for novel candidates inhibiting AR function. Herein we report that this novel triazole nucleoside analogue can inhibit AR via down-regulation of HSF1, leading to anticancer activity against CRPC.

2. MATERIALS AND METHOD

2.1 Chemistry

General: The terminal alkyne and catalysts were purchased from Acros. The microwave assisted reactions were performed on an Initiator Creator produced by Biotage. The ^1H NMR spectra were recorded at 250 MHz and the ^{13}C NMR spectra recorded at 62.5 MHz, respectively, on Bruker Avance II 250 spectrometers. The chemical shifts were recorded in parts per million (ppm). Melting points were measured with Fisher Scientific IA 9000 series digital melting point apparatus and were uncorrected. Mass analyses were performed with a QStar Elite mass spectrometer (Applied Biosystems SCIEX) equipped with a source of atmospheric pressure ionization (API) pneumatically assisted. The high resolution mass spectrum (HRMS) was obtained with a time of flight analyzer (TOF). The exact mass measurement was performed in triplicate with a double internal calibration. All compounds were purified by performing flash chromatography on silica gel (200-300 mesh). The purity of all the tested compounds were further verified by Millipore Waters (MA, USA) 1500 high performance liquid chromatography (HPLC) system with ultraviolet (UV) detector (Waters 2996). The HPLC analyses were performed using the following conditions. Method A: an analytical column of Sinochrom C18 (ELITE) (4.6 mm \times 250 mm) with an isocratic elution of $\text{CH}_3\text{OH}/\text{H}_2\text{O}$ 90/10 was used. Flow rate was 0.5 mL/min, and UV detection was set to 254 nm. Method B: an analytical column of Hypersil C8 (Agilent) (4.6 mm \times 250 mm) with an isocratic elution of $\text{CH}_3\text{OH}/\text{H}_2\text{O}$ 90/10 was used. Flow rate was 0.5 mL/min, and UV detection was set to 254 nm.

General procedure for preparing VM1-VM6

The terminal alkyne (0.24 mmol), tetrakis(triphenylphosphine)palladium(0) (11.6 mg, 0.01 mmol), CuI (1.9 mg, 0.01 mmol), Li_2CO_3 (29.6 mg, 0.4 mmol) and 5-bromo-1-[(2-hydroxyethoxy)methyl]-1,2,4-triazole-3-carboxamide (0.2 mmol) or 3-bromo-1-[(2-hydroxy-ethoxy)methyl]-1,2,4-triazole-5-carboxamide were suspended in 2.8 mL of dioxane/ H_2O (3/1) under argon. The vessel was sealed and irradiated at 100 $^\circ\text{C}$ for 25 min, and then cooled to room temperature. The reaction mixture was concentrated under reduced pressure and the crude residue was purified by flash chromatography on silica gel ($\text{CH}_2\text{Cl}_2/\text{CH}_3\text{OH}$, 20:1). The purified material was dried in vacuo to afford the corresponding products.

VM1: 66.3 mg (86 %) of product were obtained, isolated as a white solid. mp: 134.9-136.0 $^\circ\text{C}$. HPLC purity: $t = 12.24$ min, purity > 98% (method 1); $t = 12.15$ min, purity > 99% (method 2). ^1H NMR (250 MHz, CDCl_3): $\delta = 7.53$ (d, 2H, $J = 8.0$ Hz, phenyl), 7.23 (d, 2H, $J = 8.0$ Hz, phenyl), 7.11 (br s, 1H, -C(O)NH), 5.95 (br s, 1H, -C(O)NH), 5.75 (s, 2H, -NCH₂O-), 3.80-3.76 (m, 4H, -CH₂CH₂OH), 2.64 (t, 2H, $J = 7.6$ Hz, -CH₂-), 1.31-1.27 (m, 9H, -CH₂CH₂CH₂CH₃), 0.90-0.84 (m, 4H, -CH₂CH₂-); ^{13}C NMR (62.5 MHz, CDCl_3): $\delta = 160.6$, 156.2, 146.3, 132.2, 128.9, 116.8, 99.0, 78.4, 73.7, 71.8, 61.4, 36.1, 31.8, 29.2, 29.1, 22.7 ppm; IR: $\nu = 2240$ cm^{-1} (-C \equiv C-); ESI-HRMS: calcd. for $\text{C}_{21}\text{H}_{29}\text{N}_4\text{O}_3^+$ 385.2234, Found 385.2235.

VM2: 61.4 mg (53%) of product were obtained, isolated as a white solid. mp: 136.7-138.3 $^\circ\text{C}$. HPLC purity: $t = 9.35$ min, purity > 99% (method 1); $t = 7.96$ min, purity > 99% (method 2). ^1H NMR (250 MHz, $[\text{D}_6]\text{DMSO}$): $\delta = 7.97$ (br s, 1H, -C(O)NH), 7.69 (br s, 1H, -C(O)NH), 7.62 (d, 2H, $J = 8.0$ Hz, phenyl), 7.34 (d, 2H, $J = 8.0$ Hz, phenyl), 5.72 (s, 2H, -NCH₂O-), 4.71 (br s, 1H, -OH), 3.63 (t, 2H, $J = 5.0$ Hz, -CH₂CH₂OH), 3.52-3.50 (m, 2H, -CH₂CH₂OH), 2.64 (t, 2H, $J = 7.5$ Hz, -CH₂-), 1.60-1.55 (m, 2H, -CH₂-), 1.28-1.23 (m, 6H, -CH₂CH₂CH₂-), 0.85 (t, 3H, $J = 6.4$ Hz, -CH₃); ^{13}C NMR (62.5 MHz, $[\text{D}_6]\text{DMSO}$): $\delta = 159.2$, 156.3, 145.2, 139.5, 131.5, 128.5, 116.1, 96.7, 77.5, 74.0, 70.9, 59.3, 30.0, 27.7, 21.5, 13.3 ppm; IR: $\nu = 2243$ cm^{-1} (-C \equiv C-); HRMS: calcd. for $\text{C}_{20}\text{H}_{27}\text{N}_4\text{O}_3^+$ 371.2078, Found 371.2091.

VM3: mp: 132.7-133.6 $^\circ\text{C}$. HPLC purity: $t = 8.39$ min, purity > 99% (method 1); $t = 7.20$ min, purity > 99% (method 2). The characterization data was reported in reference 20[20].

VM4: mp: 134.5-135.7 $^\circ\text{C}$. HPLC purity: $t = 8.08$ min, purity > 99% (method 1); $t = 6.57$ min, purity > 99% (method 2). The characterization data was reported in reference 21 [21].

VM5: 52.5 mg (80%) of product were obtained, isolated as a white solid. mp: 124.8-126.1 $^\circ\text{C}$. HPLC purity: $t = 7.08$ min, purity > 99% (method 1); $t = 6.20$ min, purity > 99% (method 2). ^1H NMR (250 MHz, $[\text{D}_6]\text{DMSO}$): $\delta = 8.00$ (br s, 1H, -C(O)NH), 7.70 (br s, 1H, -C(O)NH), 7.59 (d, 2H, $J = 8.3$ Hz, phenyl), 7.30 (d, 2H, $J = 8.3$ Hz, phenyl), 5.69 (s, 2H, -NCH₂O-), 4.71 (t, 1H, $J = 5.5$ Hz, -OH), 3.58 (t, 2H, $J = 4.8$ Hz, -CH₂CH₂OH), 3.50-3.43 (m, 2H, -CH₂CH₂OH), 2.58 (t, 2H, $J = 7.5$ Hz, -CH₂CH₂CH₃), 1.61-1.52 (m, 2H, -CH₂CH₂CH₃), 0.85 (t, 3H, $J = 7.4$ Hz, -CH₂CH₂CH₃); ^{13}C

NMR (62.5 MHz, [D₆]DMSO): δ =159.7, 156.8, 145.5, 140.1, 132.0, 129.1, 116.6, 97.3, 78.0, 74.5, 71.4, 59.8, 37.1, 23.7, 13.5 ppm; IR: ν =2239 cm⁻¹ (-C≡C-); HRMS: calcd. for C₁₇H₂₁N₄O₃⁺ 329.1608, Found 329.1612.

VM6: 53.8 mg (70%) of product were obtained, isolated as a white solid.;mp:152.9-153.9 °C. HPLC purity: t = 13.06 min, purity > 99% (method 1); t = 10.64 min, purity > 98% (method 2). ¹H NMR (250 MHz, CDCl₃): δ =7.48 (d, 2H, J = 8.3 Hz, phenyl), 7.26 (br s, 1H, -C(O)NH), 7.14 (d, 2H, J = 8.0 Hz, phenyl), 6.01 (s, 2H, -NCH₂O-), 5.87 (br s, 1H, -C(O)NH), 3.78-3.71 (m, 4H, -CH₂CH₂OH), 2.58 (t, 2H, J = 7.6 Hz, -CH₂-), 2.35-2.00 (br s, 1H, -OH), 1.65-1.40 (m, 2H, -CH₂-), 1.30-1.10 (m, 8H, -CH₂-), 0.84 (t, 3H, J = 6.6 Hz, -CH₃); ¹³C NMR (62.5 MHz, CDCl₃): δ =157.8, 146.9, 146.4, 145.1, 132.1, 128.6, 118.2, 79.5, 78.4, 71.7, 61.5, 36.0, 31.8, 31.1, 29.2, 29.1, 22.6, 14.1 ppm. IR: ν =2240 cm⁻¹ (-C≡C-); HRMS: calcd. for C₂₁H₂₉N₄O⁺ 385.2240, Found 385.2234.

Preparation of **VM7:** 5-bromo-1-[2,3,5-tri-*O*-acetyl- β -D-ribofuranosyl]-1,2,4-triazole-3-carboxylate (92.8 mg, 0.2 mmol), the terminal alkyne (0.4 mmol), tetrakis(triphenylphosphine)-palladium(0) (11.6 mg, 0.01 mmol), CuI (3.8 mg, 0.02 mmol) and triethylamine (0.4 mL) were suspended in 3 mL of fresh distilled MeCN under argon. The vessel was sealed and irradiated at 100 °C for 30 min, and then cooled to room temperature. The reaction mixture was concentrated under reduced pressure and the crude residue purified by flash chromatography on silica gel (petroleum ether: ethyl acetate, 2:1). The purified material was dried in vacuo to afford the corresponding protected product. The protected product was then dissolved in 10 mL saturated NH₃/MeOH and stirred at room temperature for 2 days. Then the solvent was removed, the residue was dissolved in MeOH and crystallized by precipitation in CH₂Cl₂. Then the crystalline state precipitation was washed with CH₂Cl₂ and dried in vacuo to afford the corresponding product **VM7** with yield of 70%. mp:177.7-178.8°C. HPLC purity: t = 9.50 min, purity > 98% (method 1); t = 8.01 min, purity > 98% (method 2). ¹H NMR (250 MHz, [D₆]DMSO): δ =8.01 (br, 1H, -C(O)NH), 7.74 (br, 1H, -C(O)NH), 7.62 (d, 2H, J = 8.3 Hz, phenyl-H), 7.35 (d, 2H, J = 8.0 Hz, phenyl-H), 5.99 (d, 1H, J = 4.3 Hz, H-1'), 5.61 (d, 1H, J = 5.8 Hz, -OH), 5.26 (d, 1H, J = 5.8 Hz, -OH), 4.78 (t, 1H, J = 5.8 Hz, -OH), 4.49-4.55 (m, 1H, H-2'), 4.20-4.27 (m, 1H, H-3'), 3.95-4.01 (m, 1H, H-4'), 3.40-3.63 (m, 2H, H-5'), 2.65 (t, 2H, J = 7.5 Hz, -CH₂-), 1.56-1.62 (m, 2H, -CH₂-), 1.26-1.28 (m, 4H, -CH₂-), 0.83-0.89 (m, 3H, -CH₃); ¹³C NMR (62.5 MHz, [D₆]DMSO): δ =159.6, 156.9, 145.8, 140.1, 131.9, 129.0, 116.3, 97.5, 90.4, 86.2, 86.1, 74.1, 74.0, 70.5, 61.9, 35.0, 31.1, 30.5, 28.4, 28.3, 22.0, 13.8 ppm; IR: ν =2240 cm⁻¹ (-C≡C-); HRMS: calcd. for C₂₃H₃₁N₄O₅⁺ 443.2289, found 443.2284.

2.2 Biology

General: Human prostate cancer LNCaP, C4-2, 22RV-1 and PC-3 cells were purchased from American Type Culture Collection. LNCaP, C4-2 and 22RV-1 cells were grown in Roswell Park Memorial Institute 1640 (RPMI 1640) supplemented with 10% fetal bovine serum (FBS). PC-3 cells were grown in Dulbecco's Modified Eagle's Medium (DMEM) supplemented with 10% fetal bovine serum (FBS).

Cell Growth inhibition Assay

The prostate cancer cells were seeded into a 96-well plate and allowed to adhere overnight. Then the culture medium was removed and replaced with DMSO-vehicle control or containing different compounds with indicated concentration. After 48h treatment, the number of viable cells remained was determined by (3-(4,5-dimethylthiazol-2-yl)-2,5-diphenyltetrazolium bromide, MTT) colorimetric assay. All experiments were done in triplicate and repeated three independent times.

Caspase-3/7 Cleavage Assay

The prostate cancer cells were treated with the test compound for 24h, 48h and 72h. DMSO-treated cells were used as negative control. Then 100 μ L of Caspase-Glo 3/7 Assay Reagent (Promega) was added to each well of a white 96-well plate containing 100 μ L of blank, negative control cells or treated cells in culture medium. The caspase-3/7 activity was measured by the cleavage of the luminogenic substrate containing the tetrapeptide sequence DEVD according to the instructions of the manufacturer (Promega). The plate was incubated at room temperature for 1h before measuring the luminescence of each well. Each experiment was performed in triplicate.

Western Blotting Analysis

Cell lysates were prepared by suspending the cells in protein lysis buffer and subjected to routine Western blot analysis. The antibodies used for in this study included: 1:1000-diluted AR antihuman rabbit polyclonal antibody (Santa Cruz Biotechnology, Inc.), 1:500-diluted PSA antihuman goat polyclonal antibody (Santa Cruz Biotechnology, Inc.), 1:1000-diluted HSF1 antihuman rabbit polyclonal antibody (Cell Signaling Technology), 1:5000-diluted antihuman HSP27 rabbit polyclonal antibody (Stressgen Assay Designs Inc., Michigan, USA), 1:1000-diluted antihuman HSP70 rabbit polyclonal antibody (Santa Cruz Biotechnology, Inc.), 1:1000-diluted antihuman HSP90 α rabbit polyclonal antibody (Enzo Life Sciences), 1:1000-diluted antihuman AKT rabbit polyclonal antibody (Cell Signaling Technology), 1:1000-diluted antihuman cyclin D1 rabbit polyclonal antibody (Cell Signaling Technology), 1:1000-diluted antihuman p-Rb rabbit polyclonal antibody (Cell Signaling Technology) and 1:5000-diluted antihuman vinculin mouse monoclonal antibody (Sigma Chemical Co., St. Louis, MO). Specific proteins were detected using ODYSSEY IR imaging system (LI-COR Biosciences).

Quantitative Real-Time PCR (qRT-PCR)

The expression of the FKBP, NKX.3.1 and TMPRSS2 mRNAs was analyzed by quantitative Real-Time PCR amplification analysis. Total RNA was extracted from cultured cells after 24 hours of treatment using TRIzol reagent (Invitrogen). 2 μ g of total RNA was reverse transcribed using the Transcript or First Strand cDNA Synthesis Kit (Roche Applied Science). Real-time monitoring of PCR amplification of cDNA was performed using DNA primers on ABI PRISM 7900 HT Sequence Detection System (Applied Biosystems) with Tagman PCR

Master Mix (Applied Biosystems). Target gene expression was normalized to glyceraldehyde-3-phosphatedehydrogenase (GAPDH) levels in respective samples as an internal standard, and the comparative cycle threshold (C_t) method was used to calculate relative quantification of target mRNAs. Each sample was analyzed in triplicate in the PCR reaction to estimate the reproducibility of data.

Transient transfection and luciferase assay

The prostate cancer cells were allowed to adhere and proliferate overnight in 6-well plates. Then the cells were transiently co-transfected with Probasin luciferase or PSA-luciferase plasmids and control Renilla luciferase plasmids using Lipofectin (Invitrogen). The total amount of Probasin luciferase reporter or PSA plasmids DNA used were normalized to 1 μ g per well by adding control Renilla luciferase plasmids. After transfection with the plasmids, the cells were treated with **VM1** at indicated concentration and 1nM of R1881 in RPMI+10% Charcoal Stripped Serum (CSS; Invitrogen Life Technologies). 24h later, Probasin-luciferase or PSA-luciferase activities were measured using Dual-Luciferase Reporter Assay System (Promega).

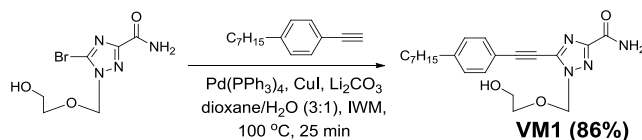
Cell-cycle analysis on Flow Cytometry

The prostate cancer cells were allowed to adhere and proliferate overnight. Culture medium was then removed and fresh media containing the indicated concentration of compound was added. No treatment was done as negative control. After 48h treatment, the cells were trypsinized and the collected cell pellet was washed with cold PBS before being fixed with 70% EtOH at 4 $^{\circ}$ C for 15 minutes. The samples were then pelleted again through centrifugation and resuspended in 500 μ L PBS containing 0.12% Triton X-100, 100 μ g/mL ribonuclease A (Sigma-Aldrich) and 50 μ g/mL Propidium iodide (Sigma-Aldrich). The samples were incubated at 37 $^{\circ}$ C for 40 minutes. Cell cycle distribution was analyzed by flow cytometry (Beckman Coulter Epics Elite, Beckman, Inc.). Each sample was performed in triplicate.

3. RESULTS AND DISCUSSIONS

3.1 Chemical synthesis

Compound **VM1** was prepared based on the established protocol [20], namely, via a microwave-assisted Sonogashira coupling reaction using 5-bromotriazole acyclic nucleoside and 1-ethynyl-4-heptylbenzene.



Scheme (1). Synthesis of compound **VM1** using microwave-assisted Sonogashira reaction.

We further synthesized compounds **VM2-VM7** (Figure 2) as the structural analogues of **VM1** for the relevant structure-activity relationship analysis (SAR) on the basis of our previous findings that the isomeric structures, different sugar

components and varying alkyl chain lengths are highly related to the anticancer activity [15, 16]. Compounds **VM2-VM5** are designated to investigate the influence of the alkyl chain length for the activity, whereas **VM6** and **VM7** are conceived for assessing the impact from the isomeric alteration in triazole ring and change of sugar component, respectively.

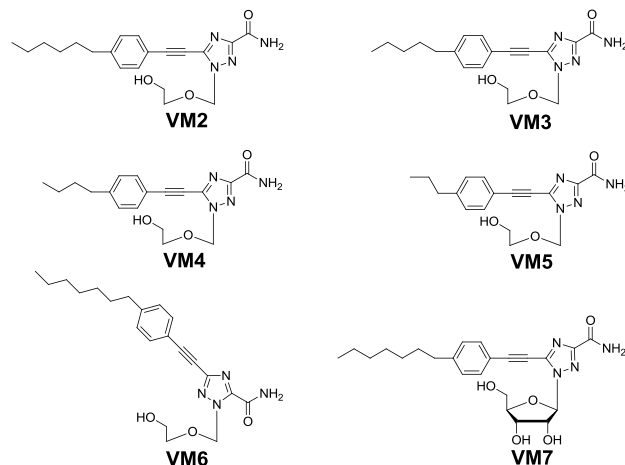


Fig. (2). The analogues of **VM1** for structure-activity relationship study.

3.2 Biological Activity

We first performed the evaluation of antiproliferation activity of the triazole nucleoside analogues using MTT assay in human prostate cancer LNCaP cells, an AR-positive and androgen sensitive cell line. Our results showed that compared to enzalutamide, the FDA-approved AR antagonist drug, **VM1** exhibited more potential antiproliferative activity in a dose-dependent manner (Figure 3A), whereas the analogues **VM2-VM5** bearing shorter alkyl chain lengths are found to be less effective (Figure 3B). In addition, neither **VM6** nor **VM7** elicited better activities compared to **VM1** (Figure 3B) indicating the importance of the 5-isomeric structure as well as acyclic sugar moiety contributes importantly to the potent activity of **VM1**. Meanwhile, **VM1** also inhibited cell proliferation of AR-positive but CRPC cell lines such as C4-2 and 22RV-1 (Figure 3C and Figure S1). Moreover, we found that **VM1** inhibited growth of AR-negative PC-3 PCa cells, although its effect was less potent than on AR-positive cells (Figure 3C and Figure S1). We further conducted apoptosis assay of **VM1** in PCa cells using caspase-3/7 activation assay. As can be seen in Figure 3D and Figure S2, the caspase-3/7 activity in cells with only 24h post-treatment increased significantly compared to DMSO-vehicle control. These results demonstrated that **VM1** was able to trigger apoptotic machinery involving in its antiproliferation activity.

As **VM1** is analogous to **Ly101-4B** and **Ly101-4B** is able to down-regulate HSF1 [16], we next determined if **VM1** also affected HSF1-mediated pathway and the related HSPs. We assessed the influence of **VM1** on the expression of HSF1 and the corresponding HSPs at protein levels using western blotting. Figure 4 showed that more than half of HSF1 protein expression was attenuated by 48h-treatment of

VM1 in LNCaP cells, which led to a dose-dependent decline of HSP27, HSP70 and HSP90 α [16]. Moreover, **VM1** also diminished the protein level of AKT, a client oncoprotein of HSPs, which further demonstrated the inhibitory activity of **VM1** on HSPs following its down-regulation of HSF1.

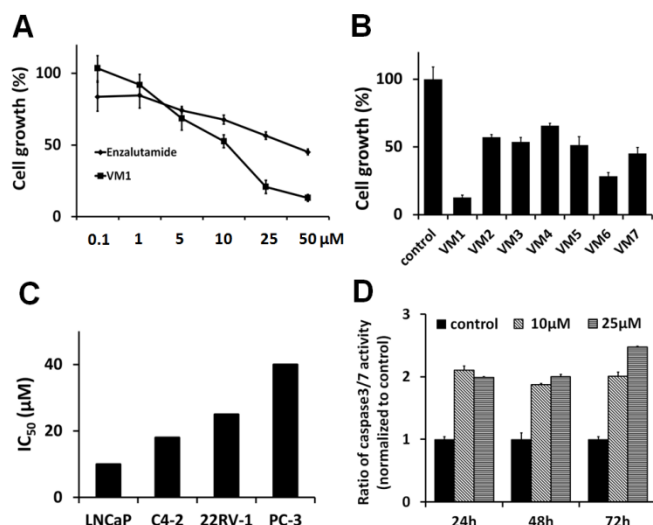


Fig. (3). Compound **VM1** inhibited cell proliferation and induced caspase-dependent apoptosis in PCa cells. (A) LNCaP cells were cultured for 48 hours in the presence of **VM1** and enzalutamide at the indicated concentration with DMSO as vehicle control. (B) Antiproliferation activity of compound **VM1-VM7** in LNCaP cells at 25 μ M. (C) IC_{50} of **VM1** in different prostate cancer cell lines. (D) Significant increase of caspase-3/7 activity following the treatment of **VM1** was determined by the cleavage of the luminogenic substrate containing the tetrapeptide sequence DEVD in LNCaP cells.

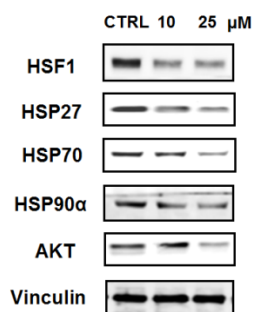


Fig. (4). Compound **VM1** down-regulates HSF1 and HSPs. LNCaP cells were treated with **VM1** at indicated concentration for 48h. Then the protein levels of HSF1, HSP27, HSP70, HSP90 α and AKT were analyzed by Western blotting using vinculin as reference.

Considering that AR requires HSPs to maintain its proper baseline folding and functions[4], various HSP inhibitors have been reported to cause perturbations of AR expression leading to significant clinical activity in PCa patients[8]. In light of the finding that **VM1** down-regulated HSF1 and HSPs expression, we then asked whether this compound could effectively modulate the expression of AR. Indeed, **VM1** reduced AR protein level in a dose- and time-

dependent manner as shown in Figure 5A. In addition to LNCaP cells, similar results on AR inhibition were obtained in C4-2 and 22RV-1 cells, confirming that **VM1** resulted in down-regulation of AR in different PCa cell lines (Figure 5A). It is noteworthy that 22RV-1 cells have high abundance of AR isoforms around 75-80 kDa compared to other AR-positive cell lines[22]. These AR isoforms have been found to be enriched in CRPCs and strongly implicated in promoting the progression to CRPC[23]. The inhibition of AR expression by **VM1** hence highlighted the potency of this compound for CRPC treatment. Given the profound activity of **VM1** in decreasing AR expression, we then assessed the influence of **VM1** on the transactivation of AR because androgenic activation of AR can lead to transcriptional activity of AR-targeted genes in association with its coregulatory factors and confer growth advantages to PCa cells[4, 24]. Figure 5B and Figure S3 showed that R1881, a synthetic androgen, highly induced AR activity. This activity was effectively suppressed by **VM1** in PCa cells as measured by Probasin and PSA luciferase assays.

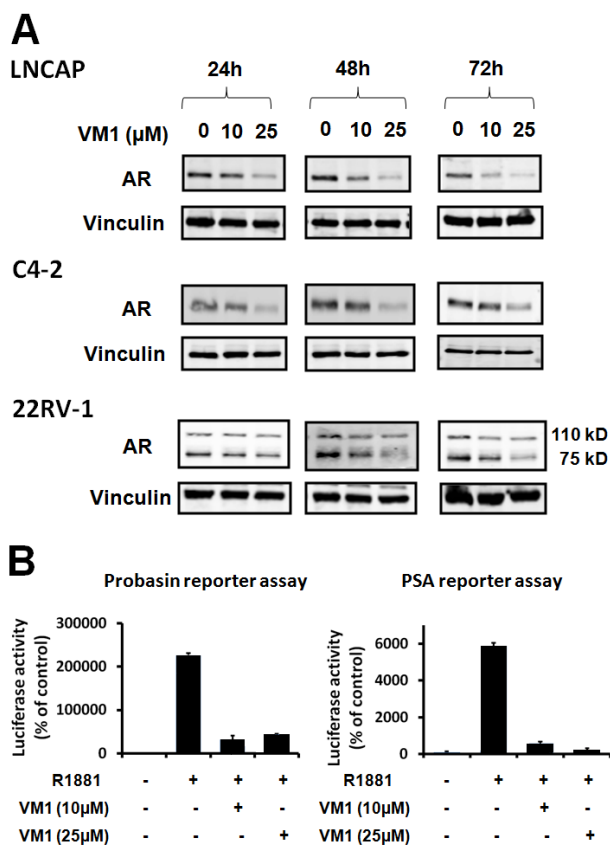


Fig. (5). **VM1** inhibits AR expression and transactivation. (A) LNCaP, C4-2 and 22RV-1 cells were treated with **VM1** for 24h, 48h and 72h, then the AR proteins level was determined by Western blotting analysis using vinculin as reference. (B) LNCaP cells were transiently transfected with Probasin-luciferase or PSA-luciferase and control renilla plasmids for 24 hours, followed by treatment of **VM1** at indicated concentration and 1 nmol/L R1881 for 12 hours in media supplemented with CSS. The luciferase activity was then determined and normalized to % of control.

Collectively, the above results therefore demonstrate an inhibitory effect of **VM1** on the constitutive AR activity.

In the AR signalling pathway, AR binds to enhancer regions of its target genes to modulate their expression. These genes are highly regulated by the expression and activation of AR. The well-characterized AR-targeted genes include PSA, FKBP5[25], NKX3.1[26] and TMPRSS2[27]. Among them, PSA is often used as biomaker for the diagnosis and monitoring of PCa. To further prove the inhibition activity of **VM1** in AR signalling pathway, quantitative real-time PCR was carried out to evaluate the mRNA level of the above mentioned AR-regulated genes after the treatment of **VM1**. As shown in Figure 6 and Figure S4, **VM1** inhibited AR transcriptional activity in a dose-dependent manner with concomitant decrease of AR dependent genes showing a decrease of PSA, FKBP5, NKX3.1 and TMPRSS2. These data suggest that **VM1** inhibits cell survival via inhibition of AR signaling pathway.

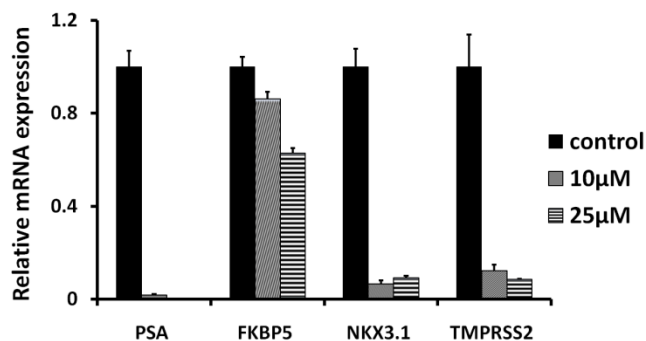


Fig. (6). LNCaP cells were treated with **VM1** for 24h. PSA, FKBP5, NKX3.1 and TMPRSS2 mRNA levels were determined by quantitative real-time PCR. mRNA levels were normalized to level of GAPDH mRNA.

The AR can also modulate cell cycle machinery and is an important regulator of cell cycle phase progression[28, 29]. Given the findings that **VM1** exerted inhibitory action on AR, we wanted to investigate whether **VM1** modulated cell cycle progression in PCa cells. We first carried out flow cytometry to examine the effect of **VM1** in different stages of cell cycle. The treatment of **VM1** led to the increase of cell fraction in SubG0 phase compared to the DMSO-vehicle control indicating the induction of apoptosis (Figure 7A and Figure S5), which is line with the results obtained from caspase-3/7 assay (Figure 3B). Moreover, the increase of cells in G0/G1 phase, alongside with the corresponding decrease of cell population in S and G2/M, affirmed that the cell cycle of the cancer cells was arrested by **VM1** (Figure 7A and Figure S5).

It has been reported that the activated AR regulates G1-S phase progression[28, 29], by stimulating G1 cyclin D accumulation as well as the phosphorylation of retinoblastoma tumor suppressor (RB) to govern the cyclin D-RB axis in PCa cells[29]. Western blotting was then performed to evaluate the expression of cell cycle proteins. As exhibited in Figure 7B and Figure S5, cells treated with **VM1** showed decreased levels of cyclin D1 and

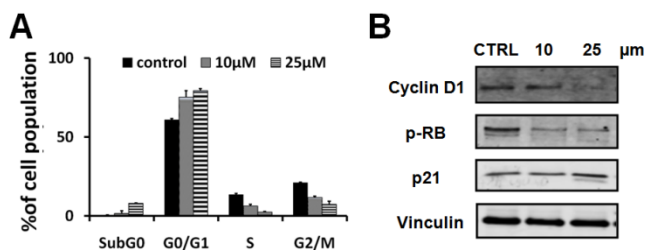


Fig. (7). Inhibition of AR by **VM1** induces cell cycle arrest. (A) LNCaP cells were treated with **VM1** for 48 h and then cells were stained with by propidium iodide. The proportion of cells in subG0, G0/G1, S, and G2/M phase was analyzed by flow cytometry. (B) LNCaP cells were treated with **VM1** for 48 h and cyclin D1, p-RB and p21 expression levels were measured by Western blotting using vinculin as reference.

phosphorylated RB protein. Additionally, **VM1** increased expression of p21, the cyclin-dependent kinase inhibitor of cell cycle[30], another marker of cell cycle arrest. Taken together, our data have demonstrated that **VM1** is effective in suppressing AR resulting in cell cycle arrest in AR-regulated phase.

CONCLUSION

In this study, we established that a novel triazole nucleoside **VM1** could effectively inhibit AR via down-regulation of HSF1 and the corresponding HSPs. The inhibition of HSF1 expression as well as AR activity by **VM1** leads to reduced expression of AR regulated genes and the induction of caspase-dependent apoptosis, leading to anticancer activity in both castration-sensitive and -resistant PCa cells. Moreover, **VM1** could efficiently arrest the cell cycle of PCa cells in AR-governed phase suggesting the potential functionality of **VM1** involved in the crosstalk between AR and cell cycle pathways.

As AR plays a central role in CRPC following androgen deprivation therapy, targeting AR remains the critical challenge in the clinical management of PCa. So far, the current AR pathway inhibitors include the CYP17 inhibitor abiraterone and the AR antagonist enzalutamide; the latter is derived from the first generation antiandrogen bicalutamide and flutamide[31]. Although nucleoside analogues are a class of clinically significant anticancer drugs for different cancers, there is no nucleoside analogue reported exhibiting anticancer activity by targeting the AR[32]. **VM1** disclosed in this work therefore presents the first synthetic nucleoside to inhibit both HSF1 and AR leading to anticancer activity in PCa and will serve as a novel structural paradigm in the search for efficacious anticancer candidates.

CONFLICT OF INTEREST

The author(s) confirm that this article content has no conflict of interest.

ACKNOWLEDGEMENTS.

We thank financial support from NIH Pacific Northwest SPORE P50 CA097186, Canceropôle PACA, INCa, CNRS and Aix-Marseille Université, the "100 talents" grant of Chongqing University (grant No. 0236011104412)

REFERENCES

- [1] Rosenthal, S. A.; Sandler, H. M. Treatment strategies for high-risk locally advanced prostate cancer. *Nat. Rev. Urol.* **2010**, *7* (1), 31-38.
- [2] Cheng, H. H.; Lin, D. W.; Yu, E. Y. Advanced clinical states in prostate cancer. *Urol. Clin. North. Am.* **2012**, *39* (4), 561-571.
- [3] Karantanos, T.; Corn, P. G.; Thompson, T. C. Prostate cancer progression after androgen deprivation therapy: mechanisms of castrate resistance and novel therapeutic approaches. *Oncogene* **2013**, *32* (49), 5501-11.
- [4] Shafi, A. A.; Yen, A. E.; Weigel, N. L. Androgen receptors in hormone-dependent and castration-resistant prostate cancer. *Pharmacol Ther* **2013**, *140* (3), 223-238.
- [5] Yuan, X.; Cai, C.; Chen, S.; Yu, Z.; Balk, S. P. Androgen receptor functions in castration-resistant prostate cancer and mechanisms of resistance to new agents targeting the androgen axis. *Oncogene* **2014**, *33* (22), 2815-25.
- [6] Friedlander, T. W.; Ryan, C. J. Targeting the androgen receptor. *Urol. Clin. North. Am.* **2012**, *39* (4), 453-464.
- [7] Shen, H. C.; Balk, S. P. Development of androgen receptor antagonists with promising activity in castration-resistant prostate cancer. *Cancer Cell* **2009**, *15* (6), 461-463.
- [8] Zoubeidi, A.; Gleave, M. Small heat shock proteins in cancer therapy and prognosis. *Int. J. Biochem. Cell Biol.* **2012**, *44* (10), 1646-1656.
- [9] Centenera, M. M.; Fitzpatrick, A. K.; Tilley, W. D.; Butler, L. M. Hsp90: still a viable target in prostate cancer. *Biochim. Biophys. Acta* **2013**, *1835* (2), 211-218.
- [10] Ischia, J.; Saad, F.; Gleave, M. The promise of heat shock protein inhibitors in the treatment of castration resistant prostate cancer. *Curr. Opin. Urol.* **2013**, *23* (3), 194-200.
- [11] He, S.; Zhang, C.; Shafi, A. A.; Sequeira, M.; Acquaviva, J.; Friedland, J. C.; Sang, J.; Smith, D. L.; Weigel, N. L.; Wada, Y.; Proia, D. A. Potent activity of the Hsp90 inhibitor ganetespib in prostate cancer cells irrespective of androgen receptor status or variant receptor expression. *Int. J. Oncol.* **2013**, *42* (1), 35-43.
- [12] Lamoureux, F.; Thomas, C.; Yin, M. J.; Kuruma, H.; Fazli, L.; Gleave, M. E.; Zoubeidi, A. A novel HSP90 inhibitor delays castrate-resistant prostate cancer without altering serum PSA levels and inhibits osteoclastogenesis. *Clin. Cancer Res.* **2011**, *17* (8), 2301-2313.
- [13] Zoubeidi, A.; Zardan, A.; Beraldi, E.; Fazli, L.; Sowery, R.; Rennie, P.; Nelson, C.; Gleave, M. Cooperative interactions between androgen receptor (AR) and heat-shock protein 27 facilitate AR transcriptional activity. *Cancer Res.* **2007**, *67* (21), 10455-10465.
- [14] Zoubeidi, A.; Chi, K.; Gleave, M. Targeting the cytoprotective chaperone, clusterin, for treatment of advanced cancer. *Clin. Cancer Res.* **2010**, *16* (4), 1088-1093.
- [15] Xia, Y.; Liu, Y.; Wan, J.; Wang, M.; Rocchi, P.; Qu, F.; Iovanna, J. L.; Peng, L. Novel triazole ribonucleoside down-regulates heat shock protein 27 and induces potent anticancer activity on drug-resistant pancreatic cancer. *J. Med. Chem.* **2009**, *52* (19), 6083-6096.
- [16] Xia, Y.; Liu, Y.; Rocchi, P.; Wang, M.; Fan, Y.; Qu, F.; Iovanna, J. L.; Peng, L. Targeting heat shock factor 1 with a triazole nucleoside analog to elicit potent anticancer activity on drug-resistant pancreatic cancer. *Cancer Lett.* **2012**, *318* (2), 145-153.
- [17] Xia, Y.; Rocchi, P.; Iovanna, J. L.; Peng, L. Targeting heat shock response pathways to treat pancreatic cancer. *Drug Discov. Today* **2012**, *17* (1-2), 35-43.
- [18] Åkerfelt, M.; Morimoto, R. I.; Sistonen, L. Heat shock factors: integrators of cell stress, development and lifespan. *Nat. Rev. Mol. Cell Biol.* **2010**, *11* (8), 545-555.
- [19] Xia, Y.; Qu, F.; Peng, L. Triazole nucleoside derivatives bearing aryl functionalities on the nucleobases show antiviral and anticancer activity. *Mini. Rev. Med. Chem.* **2010**, *10* (9), 806-821.
- [20] Zhu, R.; Wang, M.; Xia, Y.; Qu, F.; Neyts, J.; Peng, L. Arylethynyltriazole acyclonucleosides inhibit hepatitis C virus replication. *Bioorg. Med. Chem. Lett.* **2008**, *18* (11), 3321-3327.
- [21] Wang, M.; Xia, Y.; Fan, Y.; Rocchi, P.; Qu, F.; Iovanna, J. L.; Peng, L. A novel arylethynyltriazole acyclonucleoside inhibits proliferation of drug-resistant pancreatic cancer cells. *Bioorg. Med. Chem. Lett.* **2010**, *20* (20), 5979-5983.
- [22] Dehm, S. M.; Tindall, D. J. Alternatively spliced androgen receptor variants. *Endocr. Relat. Cancer* **2011**, *18* (5), R183-R196.
- [23] Waltering, K. K.; Urbanucci, A.; Visakorpi, T. Androgen receptor (AR) aberrations in castration-resistant prostate cancer. *Mol. Cell. Endocrinol.* **2012**, *360* (1-2), 38-43.
- [24] Yuan, X.; Balk, S. P. Mechanisms mediating androgen receptor reactivation after castration. *Urol. Oncol.* **2009**, *27* (1), 36-41.
- [25] Magee, J. A.; Chang, L. W.; Stormo, G. D.; Milbrandt, J. Direct, androgen receptor-mediated regulation of the FKBP5 gene via a distal enhancer element. *Endocrinology* **2006**, *147* (1), 590-598.
- [26] Tan, P. Y.; Chang, C. W.; Chng, K. R.; Wansa, K. D.; Sung, W. K.; Cheung, E. Integration of regulatory networks by NKX3-1 promotes androgen-dependent prostate cancer survival. *Mol. Cell Biol.* **2012**, *32* (2), 399-414.
- [27] Cai, C.; Wang, H.; Xu, Y.; Chen, S.; Balk, S. P. Reactivation of androgen receptor-regulated TMPRSS2:ERG gene expression in castration-resistant prostate cancer. *Cancer Res.* **2009**, *69* (15), 6027-6032.
- [28] Schiewer, M. J.; Augello, M. A.; Knudsen, K. E. The AR dependent cell cycle: mechanisms and cancer relevance. *Mol. Cell Endocrinol.* **2012**, *352* (1-2), 34-45.
- [29] Balk, S. P.; Knudsen, K. E. AR, the cell cycle, and prostate cancer. *Nucl. Recept. Signal.* **2008**, *6* e001.
- [30] Abbas, T.; Dutta, A. p21 in cancer: intricate networks and multiple activities. *Nat. Rev. Cancer* **2009**, *9* (6), 400-414.

[31] Rathkopf, D.; Scher, H. I. Androgen receptor antagonists in castration-resistant prostate cancer. *Cancer J.* **2013**, *19* (1), 43-49.

[32] Galmarini, C. M.; Popowycz, F.; Joseph, B. Cytotoxic nucleoside analogues: different strategies to

improve their clinical efficacy. *Curr. Med. Chem.* **2008**, *15* (11), 1072-1082.

Received: March 20, 2014

Revised: April 16, 2014

Accepted: April 20, 2014
